



## Modelling the mechanical behaviour of metal powder during Die compaction process

G. Cricri, M. Perrella

University of Salerno –Department of Industrial Engineering, Via Giovanni Paolo II 132, 84084. Fisciano (SA), Italy, gcricri@unisa.it; mperrella@unisa.it

**ABSTRACT.** In this work, powder compaction process was investigated by using a numerical material model, which involves Mohr-Coulomb theory and an elliptical surface plasticity model. An effective algorithm was developed and implemented in the ANSYS finite element (FEM) code by using the subroutine USERMAT. Some simulations were performed to validate the proposed metal powder material model. The interaction between metal powder and die walls was considered by means of contact elements. In addition to the analysis of metal powder behaviour during compaction, the actions transmitted to die were also investigated, by considering different friction coefficients. This information is particularly useful for a correct die design.

**KEYWORDS.** Cap-cone model; Die compaction process; FEM simulation; Residual strain.

### INTRODUCTION

A deep knowledge of metal powder behaviour during compaction stage is necessary to predict the final shape and density distribution of formed products, and to avoid damages and breakages, which may occur during the subsequent sintering phase. The design of die and of compaction process should be supported by an adequate simulation analysis of the mechanical behaviour of compacted material during the process steps. In literature, several constitutive, phenomenological and micromechanical models, based on the continuum mechanics approach, have been proposed to this aim.

In general, most used constitutive models for compaction consider the powder material as *granular* or as *porous*. Soil composed primarily of coarse-grained sand or gravel is an example of granular material, whose behaviour is strongly influenced by the friction phenomenon. Instead, constitutive equations for modelling porous materials are usually extensions of the Von Mises plasticity model, satisfying conditions of symmetry and convexity of plasticity theory. In particular, extensions of plastic flow theory, by introducing additional state variables, are used for modelling different kinds of phenomena, from creep [1] to ductile fracture [2]. For porous materials, the limit function differs from the classical one of Von Mises criterion because of incompressibility of porous solid particles during the compaction stage. Thus, the plastic flow of porous particles is considered function of two terms, at least: the hydrostatic tensor and the second principal invariant of the stress deviator tensor. For these models, the general form of the limit surface is as follows:

$$f(\sigma_{ij}) = A(\rho) \cdot J_2 + B(\rho) \cdot I_1^2 - C(\rho) \cdot K^2 \quad (1)$$



In equation (1),  $I_1$  is the first invariant of Cauchy stress tensor,  $J_2$  is the second invariant of deviatoric tensor,  $K$  is a limit stress of base material, which takes account of the hardening effect due to plastic flow, and  $A$ ,  $B$  and  $C$  are model parameters, function of variable density  $\rho$ . The simplest constitutive model combines a rule of plastic flow with an isotropic hardening law. Its basic hypothesis is to consider the powder grains only affected by plastic strains whilst their rearrangement is negligible.

Kuhn, Green, Shima, Doraivelu, Fleck and many other authors [3-16] have presented material models characterized by a yield surface function of  $I_1$  and  $J_2$ , as described in (1). However, according to Biswas [17] these relationships, developed omitting grains rearrangement mechanism, are not suitable for modelling initial stages of compaction process, at lower density levels.

Therefore, in this work a material model with two limit surfaces (*cap-cone model*) is presented in order to simulate all the die compaction steps of powders whose behaviour is both porous and granular. In such a way, it is possible to overcome the drawback highlighted by Biswas. A plastic flow law combined with friction mechanism is implemented in the finite element (FEM) commercial code ANSYS by means of the USERMAT subroutine written in Fortran. Moreover, several numerical simulations were performed to investigate the entire die compaction process, considering different friction coefficients between metal powders and die walls and punches. Friction parameters play a crucial role in the evaluation of loads applied to the die and consequently in the proper estimation of die strength and residual strains in the formed object. Therefore, these analyses are helpful for a correct die design and final recognition of formed objects' dimensions [18-20].

## MATERIAL MODEL

The material model used in this study consists of two limit surfaces [21]  $F_1$  and  $F_2$ : the former,  $F_1(\sigma)$ ,  $\theta$  is related to the Mohr-Coulomb criterion (*cone surface*); the latter,  $F_2(\sigma, \sigma_c)$ , is related to a yield elliptical surface (*cap surface*) where  $\sigma_c$  represents a hardening parameter, function of volumetric plastic strain. Such a formulation is suitable for modelling metal powders with extremely different relative density (from  $\rho_r \cong 0.2$  to  $\rho_r \cong 1.0$ ). The  $F_1$  and  $F_2$  limit surfaces are expressed in equations (2) and (3), respectively.

$$F_1(\sigma) = \frac{1}{3}I_1 \sin \varphi + \sqrt{J_2} \cos \theta - \sqrt{\frac{J_2}{3}} \sin \theta \sin \varphi - c \cos \varphi = 0 \quad \text{if } -\sigma_m < \sigma_c \quad (2)$$

$$F_2(\sigma, \sigma_c) = J_2 + M^2 \cdot \left[ (\sigma_m + \sigma_c)^2 - \left( \sigma_c + \frac{c}{\tan \varphi} \right)^2 \right] = 0 \quad \text{if } -\sigma_m \geq \sigma_c \quad (3)$$

In these equations,  $I_1$  is the first stress invariant,  $J_2$  is the second invariant of the deviatoric stress tensor and  $\sigma_m$  is the hydrostatic stress, defined as  $\sigma_m = I_1/3$ .

The yield surface  $F_1$  is obtained from the Mohr-Coulomb criterion, as a function of normal stress  $\sigma_n$  and shear stress  $\tau$ :

$$F_1 = \tau \cos \varphi + \sigma_n \sin \varphi - c \cos \varphi. \quad (4)$$

The parameters  $c$  and  $\varphi$  are respectively the cohesion and the angle of internal friction of metal powder. The angle of internal friction  $\varphi$  represents the angle of shearing resistance during compression, i.e. a measurement of resistance to relative sliding of grains. The cohesion  $c$  defines the shear strength of powder when no normal loads are applied to.

Let the principal stresses be with magnitudes  $\sigma_1 > \sigma_2 > \sigma_3$ , the equation for the surface (4) can be rewritten as (5).

$$F_1 = \frac{1}{2}(\sigma_1 - \sigma_3) + \frac{1}{2}(\sigma_1 + \sigma_3) \sin \varphi - c \cos \varphi \quad (5)$$

The principal stresses and invariants ( $I_1, J_2, \theta$ ) depend on the relationships:



$$\begin{bmatrix} \sigma_1 \\ \sigma_2 \\ \sigma_3 \end{bmatrix} = \frac{2\sqrt{J_2}}{\sqrt{3}} \begin{bmatrix} \sin(\theta + 2\pi/3) \\ \sin(\theta) \\ \sin(\theta - 2\pi/3) \end{bmatrix} + \frac{I_1}{3} \begin{bmatrix} 1 \\ 1 \\ 1 \end{bmatrix} \quad (6)$$

By using (6), the relation (5) can be expressed as a direct function of the stress invariants  $I_1$  and  $J_2$  and of the angle of Lode  $\theta$ , which describes the projection of the stress state into the deviatoric plane.

In the limit function  $F_2$ , the parameter  $\sigma_c$  controls the dimensions of the elliptical *cap surface* (Figure 1) whilst the parameter  $M$  represents the slope of the Mohr-Coulomb yield surface, in the same plane. As highlighted in Figure 1, the factor  $\sigma_c$  locates in the plane  $(\sqrt{J_2}, -\sigma_m)$  both the centre of ellipse and the ordinate of intersection of the two curves that model the overall yield surface.

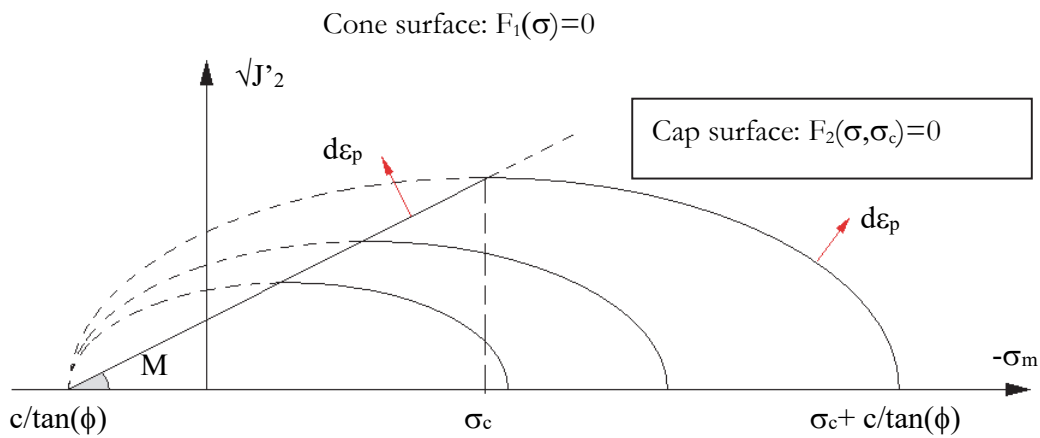


Figure 1: Cap-cone material model.

The factor  $M$  is a function of the angles  $\phi$  and  $\theta$ , as reported in eq. (7).

$$M = \sin \phi / \left( \cos \theta - \sqrt{\frac{1}{3}} \sin \theta \sin \phi \right) \quad (7)$$

The critical stress  $\sigma_c$  follows a hardening law, function of volumetric plastic strain  $\epsilon_v^p$ :

$$\sigma_c = f(\epsilon_v^p) = \sigma_{c0} \cdot e^{-\epsilon_v^p / \chi} \quad (8)$$

where  $\sigma_{c0}$  is the initial hydrostatic stress of compaction, which is obtained from considerations on the final filling of dies and assumed to be uniform, and  $\chi$  defines the plastic hardening coefficient, which is derived from a uniaxial compression/relaxation test. Thus, the limit surface has a direct dependence from plastic strain value.

The constitutive equations (*cap-cone model*) were implemented in a user defined material subroutine USERMAT of ANSYS software. The developed algorithm provides, for each increment of strain tensor, with updated stress and current constitutive tensor. Both outputs also depend on the values of state variables of constitutive law, among which the most important is the volumetric plastic strain. It controls the shape of the critical surface  $F_2$  through the hardening factor  $\sigma_c$  and other parameters. When balance convergence is satisfied for a step increment of imposed strain, all state variables' values are updated before the beginning of a new load step. In addition to relations (2)-(8), variability of elastic constants is also considered, as a function of density, and then of volumetric plastic strain, as specified in the next paragraph.



## NUMERICAL SIMULATION OF DIE COMPACTION PROCESS

### Model parameters

**M**etal powders properties are influenced by manufacturing process and chemical composition. Powders can be characterized by several parameters, including size, shape and distribution of grains, size of surface as well as flowability that influences uniform powder distribution in dies. Among powder properties, density plays a crucial role in compaction steps and affects all the parameters listed above. It can be expressed in terms of *apparent (bulk) density*  $\rho_a$ , defined as mass per unit volume of free flowing powder, or in terms of *tapped density*  $\rho_t$ , which is an increased bulk density attained after mechanically tapping a container containing the powder sample. Another parameter most used in die compaction process is *relative density*,  $\rho_r$ , i.e. degree of densification, defined as the ratio between the density of the material at a given state  $\rho$  and the density of the fully dense material  $\rho_s$ :

$$\rho_r = \frac{\rho}{\rho_s} \text{ where } \rho = \rho_0 \exp(-\varepsilon_r^p) \quad (9)$$

Pavier and Doremus [7] showed how Young's modulus, for different powder materials, highly increases as a function of relative density. They modelled such a behaviour through an exponential law. The proposed model allows calculating bulk modulus  $K$  with the following relationship:

$$K = \begin{cases} C_1 + C_2 \exp\left(C_3 \sqrt{|\varepsilon_r^p|}\right) & \text{if } I_1 < 0 \\ C_1 + C_2 & \text{if } I_1 \geq 0 \end{cases} \quad (10)$$

In particular, in this work the properties of metal powder Distaloy AE by Höganäs, mixed with 1% of Hoecht wax and 0.5% of C are used in numerical simulations. Bulk modulus  $K$  was obtained by imposing  $C_1 = 9.79$  GPa,  $C_2 = 19.35$  Pa and  $C_3 = 24.36$  in eq. (10). Successively, knowing bulk modulus  $K$  and Poisson's ratio  $\nu$ , Young's modulus is calculated by the following relationship:

$$E = 3(1 - 2\nu)K$$

Basic material properties of metal powder Distaloy AE are listed in Table 1.

Material	E [MPa]	$\nu$	K	$\rho_0$ [kg/cm <sup>3</sup> ]	$\rho_s$ [kg/cm <sup>3</sup> ]	$\chi$	$\sigma_{c0}$ [MPa]	$\phi$ [rad]
Distaloy AE	15000	0.3	12500	3.04	7.33	0.154	0.866	0.523

Table 1: Material properties of the simulated metal powder (initial values).

In powders compaction processes, shape changes are obtained by means of pressure exerted on base material by punches, which are obviously much more rigid than the material to be formed. For this reason, there is a great difference between deformations of punches and rough material. This produces a relative motion on contact surface, depending on geometry and boundary conditions at interface. The role of friction in FEM modelling of compaction is important for a proper estimation of density distribution, and even crucial in assessment of loads by pressed compact acting on dies. Friction phenomenon was evaluated considering two values of friction coefficient between metal powder and die walls:  $\mu = 0.1$ , corresponding to the average value in absence of lubricant, and  $\mu = 0.05$ , matching the average value in presence of lubricant.

### Demonstration example

As a demonstration example, numerical analysis of the stress-strain relations was performed for double action pressing process of metal powder Distaloy AE. The 2D axialsymmetric geometry considered in the calculation represents an object composed of two solid cylinders with different diameter, filleted in the middle (Figure 2).



The compaction step was simulated by using a die and two rigid punches, located at the top and bottom of the sample, which move simultaneously with different rates, in order to obtain a formed product of almost uniform density. Such working condition was considered in the numerical simulations by imposing a ratio between punches displacements that maintains average volumetric density approximately equal in upper and lower cylinder.

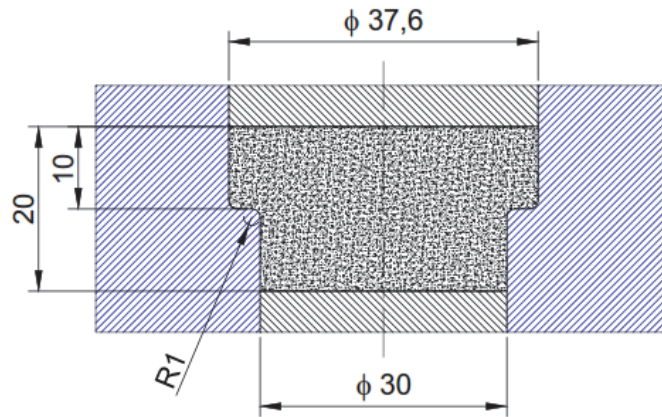


Figure 2: Geometry considered in numerical simulations.

Metal powder area was modelled with about 5000 quadratic elements PLANE183 (Figure 3). The action of punches and the friction resulting from contact both between punches and powder and between die walls and formed object were investigated by a non linear contact analysis. Die walls were modelled through TARGET169 elements whilst CONTA175 elements were used to model the perimeter of compacted component. Of course, the former elements were considered rigid respect to the latter ones.

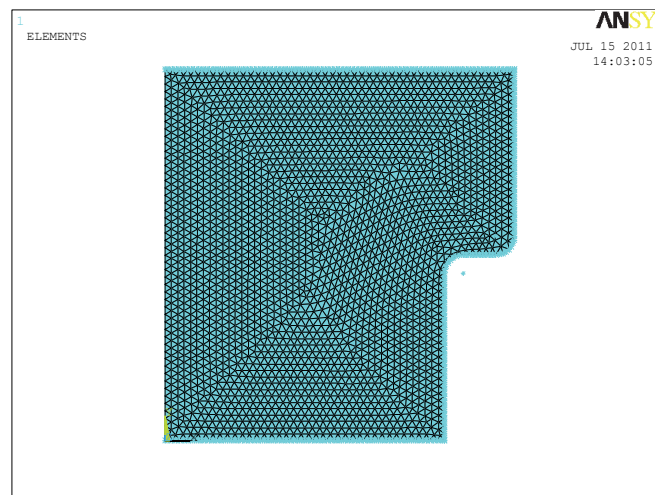


Figure 3: Axialsymmetric FE model mesh.

The trend of axial stress  $\sigma_y$  in different compaction stages is shown in Figures 4-5. It is possible to highlight that material properties and friction between metal powders and die walls cause a non-uniform stress distribution inside the specimen, with stress concentration in the filleted zones of die, as expected. Moreover, stress values become very high only in the final phase of compaction process. For the same reasons, axial stress tends to null value during the unloading step, but for the zones close to die fillets (Figure 5).

Loads transferred to dies from pressed powder is a critical factor in the compaction die design. Moreover, this information is helpful in a double way: 1) to evaluate the strain state of ejected workpiece; 2) to modify dies geometry in order to prevent errors in tolerances of formed object.

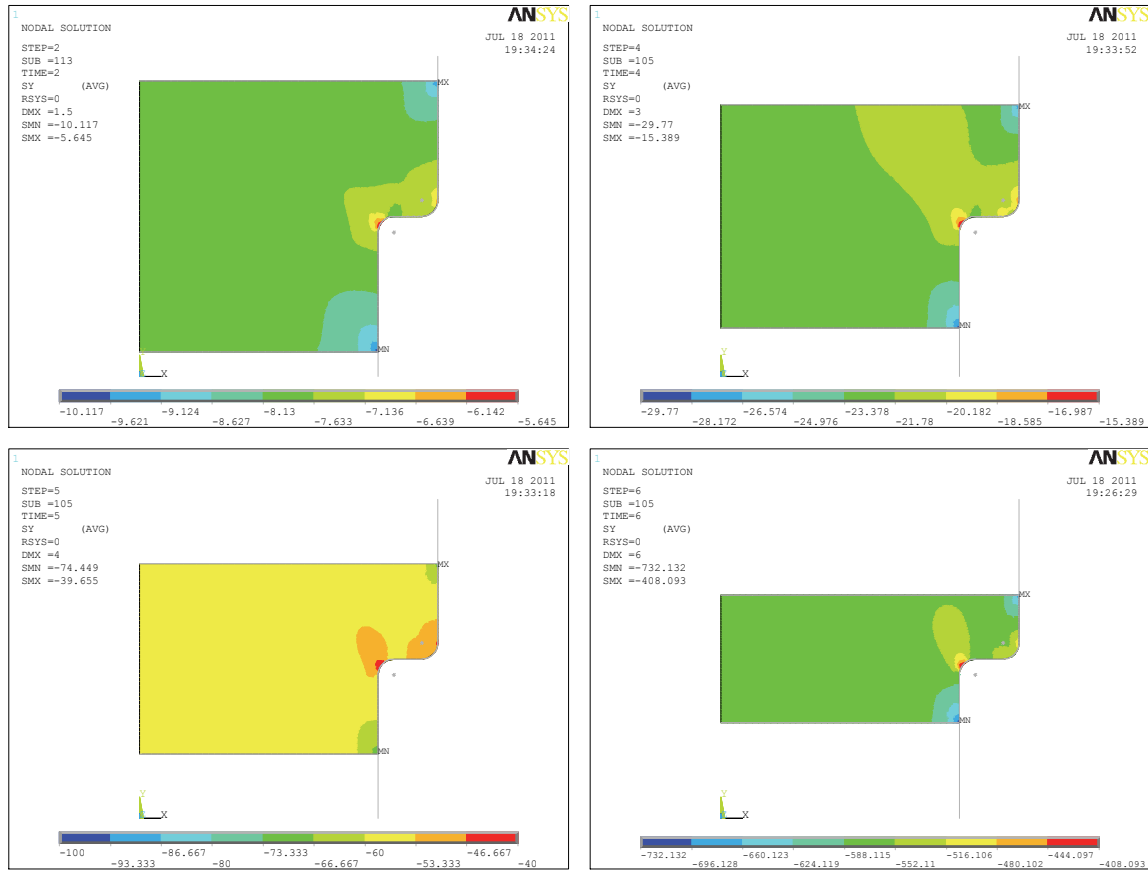


Figure 4: Axial stress  $\sigma_y$ [MPa] at different steps of compaction process (loading phase).

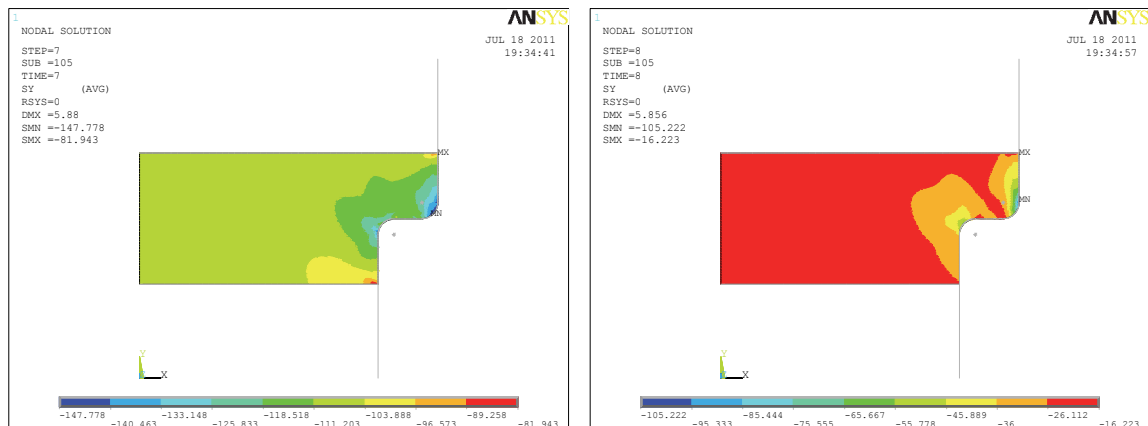


Figure 5: Axial stress  $\sigma_y$ [MPa] at different steps of compaction process (unloading phase).

In Figures 6-7 numerical results of pressure exerted by metal powder on die walls are shown, considering the step of maximum loading exerted by punches and friction coefficient equal to  $\mu = 0.1$  and  $\mu = 0.05$ , respectively. Contact pressure distribution is not uniform along surfaces of punches and die walls, because of powder mechanical behaviour, strongly influenced by local and global friction. Contact pressure exerted on upper and lower punches reaches a peak in the edges close to die walls, where friction stress is maximum, whilst presents a mean value of 570 MPa in the zones far from edges. Specifically, peak values are equal to an increase by 15% and 7% than mean outcome, when friction coefficient is  $\mu = 0.1$  and  $\mu = 0.05$  respectively.



Contact pressure applied by metal powder to the horizontal wall of die is almost equal to that exerted on punches. This is a confirmation of correct ratio of punches' displacements. Pressure on vertical walls of die varies from 290 MPa to 390 MPa (corresponding to about 50-70% of punches pressure), showing a trend almost independent of friction coefficient value. Instead, friction stress is not negligible and is strongly dependent of friction factor between powder and walls, reaching the maximum values of 57 MPa and 28 MPa when  $\mu = 0.1$  and  $\mu = 0.05$  respectively.

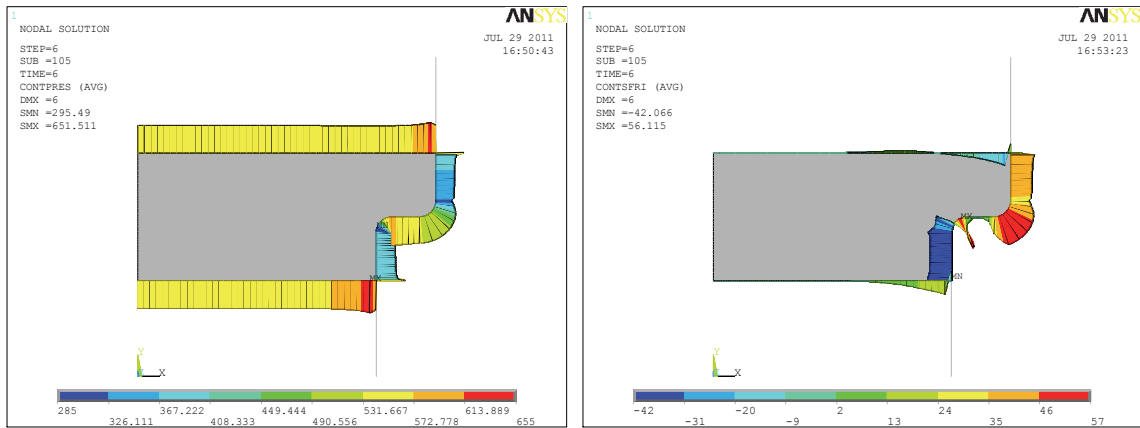


Figure 6: Contact pressure and friction stress, respectively, at final stage of compaction process, just after the loading phase ( $\mu = 0.1$ ).

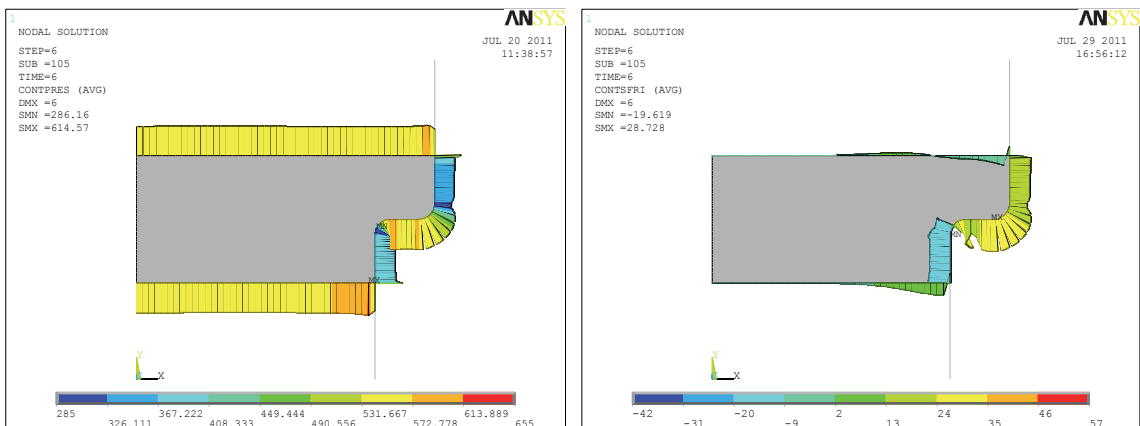


Figure 7: Contact pressure and friction stress, respectively, at final stage of compaction process, just after the loading phase ( $\mu = 0.05$ ).

The mechanical behaviour of a pressed product is function of density obtained during compaction process. Indeed, defects and failures may occur most probably in components with lower density. Moreover, for several formed elements, such as filters, the compaction level is closely connected to their correct operation.

Figure 8 shows the plot of relative density  $\rho_r$  in the final compaction scenario. The value of relative average density obtained in numerical simulations is equal to 1.075, corresponding to a final density  $\rho_s = 7.88 \text{ kg/cm}^3$ . The bulk and Young's moduli after compaction are  $K = 156 \text{ GPa}$  and  $E = 189 \text{ GPa}$  respectively. Around the corners between punches and die and in the zone of object fillets numerical analyses provide with maximum and minimum density, which are about -5.8% and + 3.5% of average density (with  $\mu = 0.1$ ) respectively.

Figure 9 depicts the variation of the minimum, maximum, and average density during the loading and unloading phases, for both considered friction coefficients. Average density is not significantly influenced by variation of friction coefficient, whilst the deviation of maximum and minimum density from the average is lower in the case with  $\mu = 0.05$  respect to the simulation with  $\mu = 0.1$ . Specifically, the previously mentioned deviation of maximum and minimum density is equal to -4.2% and +1.9% respectively.

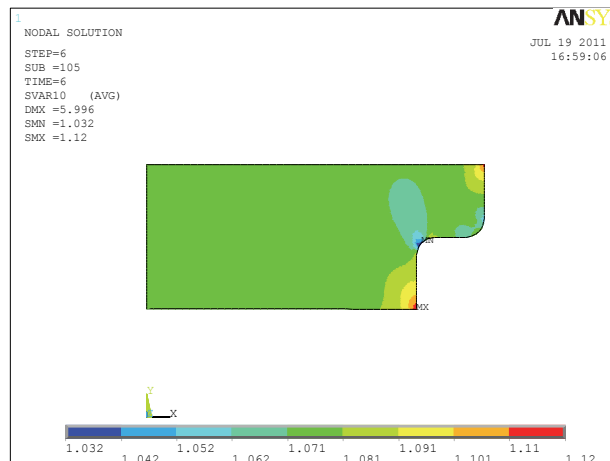


Figure 8: Relative density,  $\rho_r$  at final step of compaction process ( $\mu = 0.1$ ).

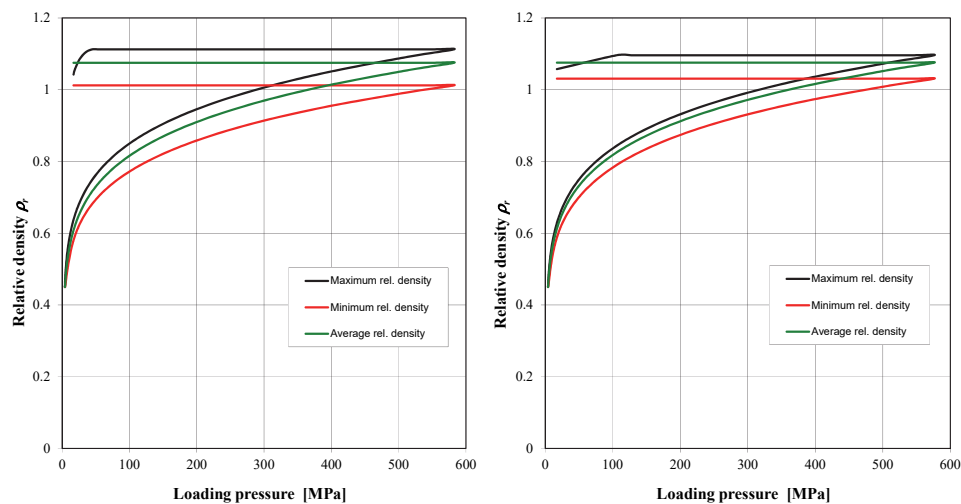


Figure 9: Relative maximum, minimum and average density vs loading pressure ( $\mu = 0.1$  and  $\mu = 0.05$ )

## CONCLUSIONS

In the present work, the behaviour of metal powder during die compaction process is described, by using a *cap-cone* model of yield surfaces in order to simulate material strain hardening capability. Material model was implemented in ANSYS FEM code by subroutine USERMAT. Several numerical simulations were performed considering a simple 2D axisymmetric geometry to evaluate the forces acting on the die walls, in addition to metal powder behaviour analysis. The obtained outcomes were used to describe an adequate characterization of the pressed object, in terms of stress and density distribution. In particular, FEM analyses highlighted that increasing friction coefficient the density gradient becomes higher and higher whilst the stress field of the compacted powders grows slowly. Although the presented constitutive material model has provided with satisfactory results, comparable with those available in literature relating to similar tests, it may be subject to further developments that make it possible to consider the relation between relative density and other parameters, such as cohesion and internal friction.

## REFERENCES

- [1] Cali, C., Cricri, G., Perrella, M., An advanced creep model allowing for hardening and damage effects, *Strain*, 46-4 (2010) 347-357. DOI: 10.1111/j.1475-1305.2009.00682.x





- [2] Cricri, G., A consistent use of the Gurson-Tvergaard-Needleman damage model for the R-curve calculation, *Frattura ed Integrità Strutturale*, 24 (2013) 161-174. DOI: 10.3221/IGF-ESIS.24.17
- [3] Green, R.J., A plasticity theory for porous solids, *Int. J. Mech. Sci.* 14 (1972) 215-224.
- [4] Kuhn, H.A., Downey, C.L., Deformation characteristics and plasticity theory of sintered powder materials, *Int. J. Powder Metall.*, 7-1 (1971) 15-25.
- [5] Doraivelu, S.M., Gegel, H.L., Gunasekera, J.S., Malas, J.C., Morgan, J.T., Thomas Jr., J.F., A new yield function for compressible PM materials, *Int. J. Mech. Sci.*, 26-9/10 (1984) 527-535.
- [6] Shima, S., Oyane, M., Plasticity theory for porous metals, *Int. J. Mech. Sci.* 18 (1976) 285-291.
- [7] Pavier, E., Doremus, P., Triaxial characterisation of iron powder behaviour, *Powder Metallurgy*, 42-4 (1999) 345-352.
- [8] Fleck, N.A., Kuhn, L.T., McMeeking, R. M., Yielding of metal powder bonded by isolated contacts, *J. Mech. Phys. Solids*, 40-5 (1992) 1139-1162. DOI: 10.1016/0022-5096(92)90064-9
- [9] Carnavas, P.C., Page, N.W., Elastic properties of compacted metal powders, *Journal of Materials Science*, 33 (1998) 4647-4655.
- [10] Jonsen, P., Häggblad, H.-Å., Modelling and numerical investigation of the residual stress state in a green metal powder body, *Powder Technology*, 155 (2005) 196-208. DOI: 10.1016/j.powtec.2005.05.056
- [11] Lewis, R.W., Khoei, A.R., A plasticity model for metal powder forming processes, *International Journal of Plasticity*, 17 (2001) 1659-1692. DOI: 10.1016/S0749-6419(00)00096-6
- [12] Khoei, A.R., Numerical simulation of powder compaction processes using an inelastic finite element analysis, *Materials and Design*, 23 (2002) 523-529.
- [13] Chtourou, H., Guillot, M., Gakwaya, A., Modelling of the metal powder compaction process using the cap model. Part. I. Experimental material characterization and validation, *International Journal of Solids and Structure*, 39 (2002) 1059-1075. DOI: 10.1016/S0020-7683(01)00255-4
- [14] Park, S.J., Han, H.N., Oh, K.H., Lee, D.N., Model for compaction of metal powders, *International Journal of Mechanical Sciences*, 41 (1999) 121-141.
- [15] Smith, L.N., Midha, P.S., Graham, A.D., Simulation of metal powder compaction, for the development of a knowledge based powder metallurgy process advisor, *Journal of Materials Processing Technology*, 79 (1998) 94-100.
- [16] Bocchini, G.F., Criteri di classificazione del grado di complicazione delle forme dei componenti sinterizzati, *La Metallurgia Italiana*, 7 (2008) 37-44.
- [17] Biswas, K., Comparison of various plasticity models for metal powder compaction processes, *J. of Material Processing Technology*, 166 (2005) 107-115. DOI: 10.1016/j.jmatprotec.2004.08.006
- [18] Bocchini, G.F., Cricri, G., Esposito, R., Influence of operating temperature on shrink fitting pressure of PM dies, *Powder Metallurgy*, 39-3 (1996) 195-206.
- [19] Armentani, E., Bocchini, G.F., Cricri, G., Esposito, R., Short dies and thin walled inserts for room temperature or warm compaction - numerical determination of design features, *Powder Metallurgy*, 45-2 (2002) 115-133.
- [20] Armentani, E., Bocchini, G.F., Cricri, G., Esposito, R., Metal powder compacting dies: Optimised design by analytical or numerical methods, *Powder Metallurgy*, 46-4 (2003) 349-360.
- [21] Lewis, R.W., Khoei, A. R., Numerical modelling of large deformation in metal powder forming, *Comput. Methods Appl. Mech. Engrg.*, 159 (1998) 291-328.